# The Saxophone by Model and Measurement

**Tamara Smyth**
School of Computing Science,
Simon Fraser University
tamaras@cs.sfu.ca

**Srikanth Cherla**
School of Computing Science,
Simon Fraser University
scherla@cs.sfu.ca

## ABSTRACT

This work presents an extension to a measurement technique used to estimate the reflection and transmission functions of musical instrument bells within the context of parametric waveguide models. In the original technique, several measurements are taken of a system—a 2-meter long cylindrical tube with a speaker and co-located microphone at one end and incrementally varying termination conditions at the other. Each measured impulse response yields a sequence of multiple evenly spaced arrivals from which estimates of waveguide element transfer functions, including the bell reflection and transmission, may be formed.

Use of this technique to measure a complete saxophone presents a number of difficulties stemming from the fact that the bell is not easily separated from the bore for an isolated measurement. The alternative of appending the complete saxophone yields a measured impulse response where 1) echos overlap in time and are not easily windowed and 2) the presence of a junction between measurement tube and saxophone cause spectral artifacts. In this work we present an alternate post-signal-processing technique to overcome these difficulties, while keeping the hardware the same. The result is a measurement of the saxophone's round-trip reflection function from which its transfer function, or its inverse—the impulse response, may be constructed.

## 1. INTRODUCTION

It is well known that wave propagation in wind instrument bores may be modeled in one dimension using the waveguide structure shown in Figure 1, with a bi-directional delayline accounting for the acoustic propagation delay in a cylindrical or conical bore section, filter elements $\lambda_N(z)$, $R_{mp}(z)$ accounting for the propagation loss, and reflection at the mouthpiece, respectively, and elements $R_B(z)$ and $T_B(z)$ describing the reflection and transmission functions of the bell, the non-cylindrical/non-conical section at the end of the instrument [1]. If $R_B(z)$ and $T_B(z)$ are permitted to have "long-memory" acoustic information, this model is also valid for instruments having toneholes, with open tonehole radiation and scattering being lumped into $R_B(z)$ and $T_B(z)$.

In this work, a parametric model of a saxophone without toneholes is presented following Figure 1, where the bore resonance may be set according to the pure delay $z^{-N}$, and where $R_B(z)$ and $T_B(z)$ hold solely the acoustic behaviour of the bell. As wave propagation within horns (shapes not purely cylindrical / conical) involves higher-order and evanescent modes, a one-dimensional model cannot capture the complete behaviour of this instrument section, and a more accurate description of $R_B(z)$ and $T_B(z)$ is expected through measurement. Several techniques exist for measuring acoustic properties of wind instrument bores [2–9], most often in the acoustic community in terms of its input impedance. The technique here focuses on the use of low-cost hardware and a simple setup, with acoustic information being estimated using post-signal-processing of measured impulse responses.

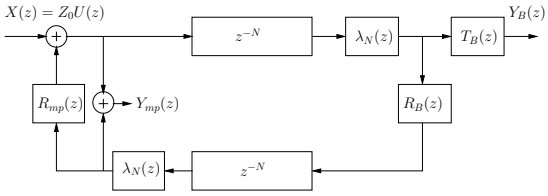


**Figure 1**. Waveguide model of a cylindrical/conical bore section with commuted propagation loss filters $\lambda_N(z)$, bell reflection and transmission filters $R_B(z)$ and $T_B(z)$ respectively, and a reflection filter $R_{mp}(z)$ at the bore base corresponding to the position of the mouthpiece/reed. The instrument transfer function corresponding to observation point $Y_{mp}(z)$ is given by (4) in response to input pressure $X(z) = Z_0U(z)$, where $Z_0$ is the characteristic impedance and $U(z)$ is the volume flow through the reed.

The authors acquired a tenor saxophone without toneholes and chimneys, an instrument typically used by saxophonists wishing to practice solely embouchure and blowing techniques. For the sake of this work and validating results, measurements are taken of both the complete instrument as well as just the bore, with the bell removed (a considerably easier task when there is no hardware on the instrument). In the latter case, the bore is considered to be conical and thus reasonably modeled as a one-dimensional waveguide, providing a basis for validating the estimation results. Any measured losses for either device under test (DUT) are assumed to be due to propagation loss $\lambda_N(z)$ and a termination: an open end for the cone (the well-described open cylinder reflection provides a reasonable approximation for the open cone), and the bell reflection $R_B(z)$ and transmission $T_B(z)$ for the complete instrument. To measure the instrument and these losses, a previ-

ously presented technique used for estimating bore terminations from measurement [10] is further developed, with additional (and alternate) post signal processing to handle an entire instrument, i.e. one where 1) the bell does not easily separate from the bore, 2) the device of the test is too long to produce isolated echos in the measured impulse response, and 3) the junction created by appending the device under test to the measurement tube creates a reflection inconsistent with that of a bore base.

## 2. MEASUREMENT SYSTEM

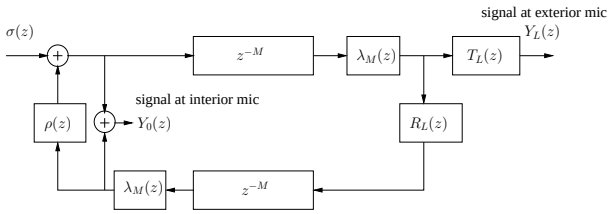


**Figure 2**. Waveguide model of the measurement system: a 2-meter long tube with a speaker and co-located microphone at one end, and an incrementally varying termination at the opposite end: closed then with a device under test (DUT) appended, creating a reflection $R_L(z)$ and a transmission $T_L(z)$. The speaker transmission is described by $\sigma(z)$ and the reflection off the speaker is described by $\rho(z)$.

The original measurement technique being employed here is fully described in [10], and involves estimating wind instrument waveguide elements from several measurements of the systems impulse response. The measurement system, the waveguide model of which is shown in Figure 2, consists of a 2-meter long tube with a speaker and co-located microphone at one end, enabling both an input driving signal $\sigma(\omega)$ and a simultaneous measurement $Y_0(\omega)$ at approximately the same position in the measurement tube. Each measurement is of the system having incrementally varying termination/boundary conditions: first the tube is closed, then open, and finally it is appended with a device under test (DUT). When the DUT is sufficiently short (as compared to the measurement tube), each measured impulse response yields a sequence of multiple sufficiently spaced arrivals, from which estimates of waveguide element transfer functions (those elements shown in Figure 2) may be formed.

Following the round-trip propagation of the signal in the measurement system, shown in Figure 2, from speaker / microphone to the opposite termination and back again, it may be seen that the spectral composition of the second arrival of the measured impulse response corresponding to $Y_0(z)$ is given by

$$Y_{0,2}(\omega) = \sigma(\omega)\lambda^2(\omega)R_L(\omega)(1+\rho(\omega)), \qquad (1)$$

where $\sigma(\omega)$ is the speaker transfer function, $\rho(\omega)$ is the reflection off the speaker, and $R_L(z)$ is the reflection function of the terminating condition (for a closed tube, $R_L(z) = 1$). Equations expressed as a function of $\omega$ signify the use of measured data.

Since the technique involves taking multiple measurements of the system, one with the tube closed, and one with a different termination (either open or with an appended DUT), it is shown in [10] that the reflection of the terminating condition $R_L(z)$ may be estimated by taking the spectral ratio of second arrivals

$$\hat{R}_L(\omega) = \frac{\sigma(\omega)\lambda^2(\omega)R_L(\omega)(1+\rho(\omega))}{\sigma(\omega)\lambda^2(\omega)(\omega)(1+\rho(\omega))}, \qquad (2)$$

where the numerator describes the spectrum of the second arrival for the tube with termination reflection $R_L(z)$, and the denominator describes the spectrum of the second arrival for the closed tube.

In [10], the measurement and post-signal-processing technique is explored using simple structures consisting of cylindrical and conical tubes, as these are well described theoretically and provide a basis for validating data estimated from measurement. Shown to yield data closely matching the theory, the technique is later extended to measure structures which are more difficult to describe theoretically, such as an instruments flaring bell. In [11], the technique is used to obtain the transfer function of the clarinet bell by appending the bell to the measurement tube and taking the spectral ratio given by (2), to improve a clarinet synthesis model which uses the "generalized pressure-controlled valve". In [12], it was shown that though a trombone bell could be measured by appending the bell to the end of the measurement tube and applying (2), improved results are obtained by adapting the measurement post processing to account for the discontinuity created when the appended bell has a small-end radius different from the inner radius of the measurement tube.

In this work, further modification is required to make this system useful for measuring features of the saxophone. This application, which involves estimating the *complete* instrument transfer functions $H_{mp}(z) = Y_{mp}(z)/X(z)$ and $H_L(z) = Y_L(z)/X(z)$ (see Figure 1), instead of solely the reflection and transmission functions $R_B(z)$ and $T_B(z)$ of the bell, presents difficulties requiring a change in the signal post-processing approach (the hardware setup remains the same).

Firstly, unlike the clarinet and trombone bells, the saxophone bell is not easily removed from the instrument. Thus, the saxophone bell cannot be appended to the measurement tube to obtain its transfer function $R_B(z)$. Rather, the measurement must be of the whole instrument, with both bore and bell as a single unit, and no clear separation between the two. Furthermore, the saxophone transfer function cannot be obtained by taking the ratio of second arrivals (as was done for instrument bells), because appending the entire saxophone to the end of the two-meter tube results in a measured impulse response with no clear separation between arrivals/echos. Thus, windowing to extract the second arrival, as was done in [10–12], is not straightforward and taking the spectral ratio given by (2) is significantly more difficult. Lastly, appending the saxophone to the measurement tube creates a discontinuity (though not a leak) between tube and DUT radii and a junction between cylindrical and conical structures. A measurement of the instrument transfer function obtained by taking the spectral ratio of second arrivals (2), if it were

possible to extract the second arrival, would include the reflection off the junction ($R_2(z)$ in Figure 4). This inclusion would present an artifact when trying to fit the estimated transfer function to the waveguide model of the instrument (Figure 1). Though the inclusion of $R_2(z)$ is acceptable when measuring solely the bell, since $R_2(z)$ is relatively close to the reality of the junction (and reflection) created by appending a bell to a bore, it is not acceptable when that position corresponds to that of the mouthpiece. Since reflection $R_2(z)$ and the expected reflection off a typical reed / mouthpiece are significantly different (the former being predominantly open, the latter being predominantly closed), it is desirable to omit $R_2(z)$ when estimating the transfer function for an entire instrument. If the junction reflection is omitted in the estimation, the instrument transfer function can be constructed, as discussed below in Section 3, with a reflection $R_{mp}(z)$ that is more consistent with the termination of the bore (either cylindrical or conical), when coupled to reed / mouthpiece.

For this reason, we present further modification to the original signal-post-processing technique, enabling estimation of the round-trip reflection function of the saxophone from the measurement system's impulse response (corresponding in the $z$-domain to $Y_0(z)$ in Figure 2). The reflection function is then used to fit a waveguide model having a more appropriate $R_{mp}$, ultimately yielding the instrument's transfer function corresponding to $Y_{mp}(z)/X(z)$.

## 3. INSTRUMENT TRANSFER FUNCTION

Given the waveguide model in Figure 1, the corresponding round-trip reflection function of the saxophone instrument, from the mouthpiece to the bell and back again, is given by

$$R_I(z) = R_B(z)\lambda_N^2(z)z^{-2N}. \tag{3}$$

The instrument transfer function corresponding to the ratio of the pressure at the reed / mouthpiece $Y_{mp}(z)$ to input pressure $X(z)$ (the inverse-transform of which yields the sequence of arrivals making up the instrument impulse response) is given by

$$\begin{aligned} H_{mp}(z) &= \frac{Y_{mp}(z)}{X(z)} \\ &= \frac{1 + R_B(z)\lambda_N^2(z)z^{-2N}}{1 - R_{mp}(z)R_B(z)\lambda_N(z)^2 z^{-2N}}, \end{aligned}$$

which can also be expressed in terms of (3) as

$$H_{mp}(z) = \frac{1 + R_I(z)}{1 - R_{mp}(z)R_I(z)}. \tag{4}$$

Thus, an estimation of the round-trip instrument reflection function $R_I(z)$ from measurement, would allow for construction of the instrument transfer function (4), and a fit to the waveguide model in Figure 1, using a mouthpiece reflection $R_{mp}(z)$ that is more suitable to the termination of the cylindrical / conical bore coupled to a reed model. The pure delay $z^{-2N}$ may be made parametric so that it may be set according to a desired pitch.

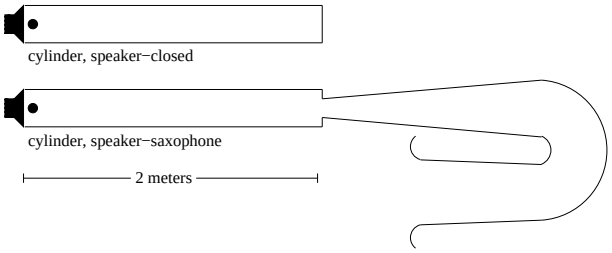


**Figure 3**. The measurement system consisting of a 2-meter tube with a speaker and co-located microphone at one end. The tube is measured first closed (top), then with a saxophone appended (bottom) to produce the measurement's impulse response under both terminating conditions.

### 3.1 Estimating $R_I$ from the measurement system

Though the system created by appending the saxophone to the measurement tube may be approximately modeled by Figure 2, a more realistic model is given in Figure 4, where the connection between tube and saxophone creates a change of wave impedance at the boundary between cylindrical and conical tubes, resulting in reflection

$$R(\omega) = \frac{Z_2(\omega)/Z_1(\omega) - 1}{Z_2(\omega)/Z_1^*(\omega) + 1} \tag{5}$$

between adjacent wave impedances $Z_1$ and $Z_2$ (where * indicates the complex conjugate), and an amplitude complementary transmission

$$T(\omega) = 1 + R(\omega). \tag{6}$$

For spherical pressure waves in conical tubes (as denoted by the $n$ subscript) propagating away from the cone apex (denoted by the $+$ superscript), the impedance is dependent on frequency $\omega$ and the distance $r$ from the observation point to the cone apex, and is given by

$$Z_n^+(r;\omega) = \frac{\rho c}{S_n}\frac{j\omega}{j\omega + c/r}, \tag{7}$$

where $S_n$ is the cross-sectional area of the cone's smaller end (at the junction), and $c$ is the wave propagation speed. For spherical waves propagating toward the cone apex, the impedance is given by

$$Z_n^-(r;\omega) = \frac{\rho c}{S_n}\frac{j\omega}{j\omega - c/r} = Z_n^+ * (r;\omega). \tag{8}$$

For cylinders (as denoted by the $y$ subscript), the distance $r$ approaches infinity and the $c/r$ term becomes negligible, yielding a wave impedance given by

$$Z_y = \frac{\rho c}{S_y}. \tag{9}$$

The reflection function $R_1(z)$ describing the pressure returning to the cylindrical tube is thus given by

$$R_1(\omega) = \frac{Z_n^+/Z_y - 1}{Z_n^+/Z_y + 1}, \tag{10}$$

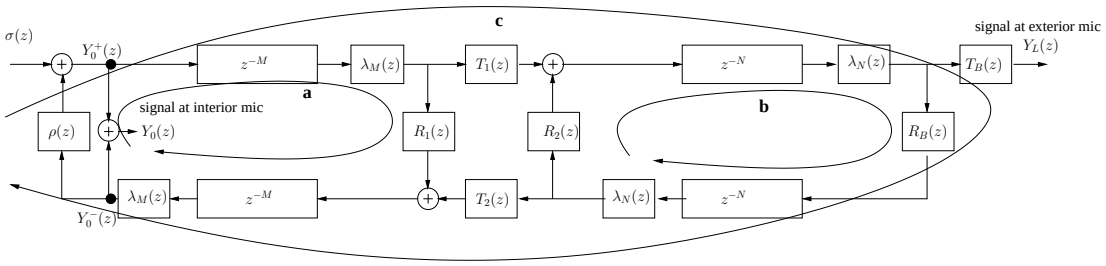


**Figure 4**. Given the discontinuity between the measurement tube and the appended saxophone with cross-sectional areas $S_y$ and $S_n$, respectively, the measurement system consists of a 2-port scattering junction, with reflection $R_{1,2}$ and transmission $T_{1,2}$, described by (5-11).

and the reflection function $R_2(z)$ describing the pressure returning to the cone is given by

$$R_2(\omega) = \frac{Z_y/Z_n^- - 1}{Z_y/Z_n^{-*} + 1}. \tag{11}$$

If $S_y = S_n$, then $R_1(z) = R_2(z)$, and the reflection at the junction reduces to

$$R_1(\omega) = R_2(\omega) = \frac{-1}{1 + 2j\omega r/c}, \tag{12}$$

a one-pole low-pass filter with a cutoff frequency of $\omega = c/r$.

The transfer function of the entire measurement system shown in Figure 4, corresponding to the ratio of the measured signal $Y_0(z)$ to the input speaker transfer function $\sigma(z)$, is given by

$$\begin{aligned} H_0(z) &= \frac{Y_0(z)}{\sigma(z)} \\ &= \frac{1 + b_M z^{-2M} + b_N z^{-2N} + b_{M,N} z^{-2(M+N)}}{1 + a_M z^{-2M} + a_N z^{-2N} + a_{M,N} z^{-2(M+N)}}, \end{aligned} \tag{13}$$

where the feedforward coefficients are given by

$$\begin{aligned} b_M &= R_1 \lambda_M^2, \\ b_N &= -R_2 R_B \lambda_N^2, \\ b_{M,N} &= -\left(R_1 R_2 - T_1 T_2\right) R_B \lambda_M^2 \lambda_N^2, \end{aligned}$$

and the feedback coefficients are given by

$$\begin{aligned} a_M &= -\rho R_1 \lambda_M^2, \\ a_N &= -R_2 R_B \lambda_N^2, \\ a_{M,N} &= \rho\left(R_1 R_2 - T_1 T_2\right) R_B \lambda_M^2 \lambda_N^2, \end{aligned}$$

where all waveguide elements are functions of $z$ (as in Figure 4), but omitted for brevity. The derivation of (13) is shown in Appendix A.

Conveniently, equation (13) can also be expressed in terms of the round-trip reflection of the closed measurement tube,

$$R_{cl}(z) = \lambda_M^2(z) z^{-2M}, \tag{14}$$

and the round-trip reflection function $R_I(z)$ of the appended instrument (3),

$$H_0(z) = \frac{1 + R_1 R_{cl} - R_2 R_I - (R_1 R_2 - T_1 T_2) R_{cl} R_I}{1 - \rho R_1 R_{cl} - R_2 R_I + \rho (R_1 R_2 - T_1 T_2) R_{cl} R_I}. \tag{15}$$

### 3.2 Estimating $\hat{R}_I$ from measurement

Estimating the round-trip instrument reflection $\hat{R}_I(z)$ is done by first taking a measurement of the tube with a closed termination. Following the steps described in [10] allows for estimation of speaker transmission $\sigma(\omega)$, the reflection off the speaker $\rho(\omega)$, and the propagation loss of the measurement tube $\lambda_M(\omega)$, or alternatively, an estimation of the lumped round-trip reflection function for the closed tube $\hat{R}_{cl}$, given in (14).

A second measurement, taken with the saxophone instrument appended to the measurement tube, produces an impulse response, the transform of which yields $Y_0(\omega)$, that when divided by the speaker speaker transfer function $\sigma(\omega)$ yields $H_0(\omega)$, a measurement of (15). Given the closed tube reflection function estimate $\hat{R}_{cl}(\omega)$ made from the prior closed tube measurement, the round-trip instrument reflection function can be estimated by

$$\hat{R}_I(\omega) = \frac{1/R_2(\omega) + \zeta R_1(\omega) \hat{R}_{cl}(\omega)}{1 + \zeta \left(R_1(\omega) R_2(\omega) - T_1(\omega) T_2(\omega)\right) \hat{R}_{cl}(\omega)}, \tag{16}$$

where

$$\zeta = \frac{1 + \rho(\omega) H_0(\omega)}{R_2(\omega)(1 - H_0(\omega))}. \tag{17}$$

The saxophone instrument transfer function is then constructed using (4), with $R_{mp}$ set using the closed-end reflection of a truncated cone (i.e. a boundary condition where the volume velocity is equal to zero), given by

$$R_{mp}(\omega) = \frac{Y_0^+(\omega)}{Y_0^-(\omega)} = \frac{Z_n^+(r;\omega)}{Z_n^-(r;\omega)} = \frac{j\omega - c/r}{j\omega + c/r}. \tag{18}$$

### 3.3 Results

The estimation technique is first applied to a case where a short large closed cylinder is appended to the measurement tube. As the propagation loss in a cylinder is well-described theoretically, it provides a good basis for validating the transfer function given by (13) in the presence of a junction with real-valued reflection and transmission functions, and the estimation of (16). In both cases, as shown in Figure 5, measurement and estimation show a good match with theoretical expectation.

The next case is of the sax conical bore (with bell removed) appended to the measurement tube. As shown in Figure 6 (top), the measurement of the system (tube + conical bore) shows good agreement with its theoretically constructed counterpart. The theoretical round-trip reflection

$R_I$ of the conical section is constructed with an open-end cylindrical reflection, yet as shown in Figure 6 (bottom), there is still good agreement with estimated $\hat{R}_I$.

The final case is of the complete saxophone (with bell) appended to the measurement tube. Figure 7 illustrates the effects of the saxophone bell as compared to the results of the saxophone conical bore (without bell). As seen in Figure 7 (top), the bell shifts the resonant peaks in the spectrum and (bottom) contributes an increased low-pass characteristic.

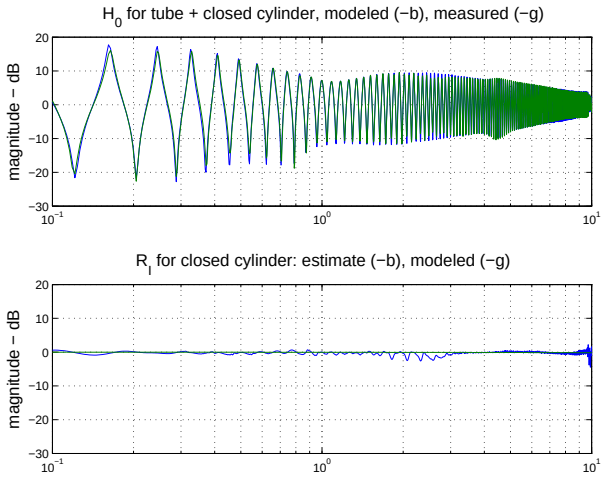


**Figure 5**. A measurement taken of the 2-meter tube with a closed cylinder appended (green), is plotted along with a theoretically constructed model (blue), with the two showing good agreement (top). A strong match is also observed for the theoretically constructed round-trip reflection function $R_I(\omega)$ of a closed cylinder (green) and that estimated from measurement using (16) (blue).

## 4. CONCLUSION

In this work, the measurement and post-signal-processing technique first presented in [10], and later in [11] for measurement of a clarinet bell, and in [12] for measurement of the bell of a trombone, is modified to accommodate the slightly different task of measuring the *complete* instrument transfer function of a saxophone.

The use of the technique for measuring the saxophone presents difficulties due to 1) the fact that the bell does not separate from the bore and cannot be measured in isolation, 2) the length of the saxophone causes an undesirable overlapping in the measured impulse response echos from which waveguide elements are formed, and 3) the presence of a junction when appending the saxophone to the measurement tube creating spectral "artifacts". This work presents a modified approach to the post-signal-processing technique needed to overcome these difficulties, while keeping the hardware component of the measurement system the same.

The resulting strategy is to estimate the saxophone's round-trip reflection function $\hat{R}_I(\omega)$ from a measurement of the system (tube + DUT), and using $\hat{R}_I(\omega)$ to construct the instrument transfer function—the inverse transform of which yield's the instrument's impulse response. Since it is difficult to validate the technique with actual saxophone data, a validation is first made using an appended cylinder and then a cone (the conical bore of the saxophone with the bell removed), both DUTs being well-described theoretically. The results shown in Figures 5 and 6 provide confidence that the estimation technique is producing good results, and may be applied to a saxophone bore and bell, the results of which, shown in Figure 7, are consistent with expectation.

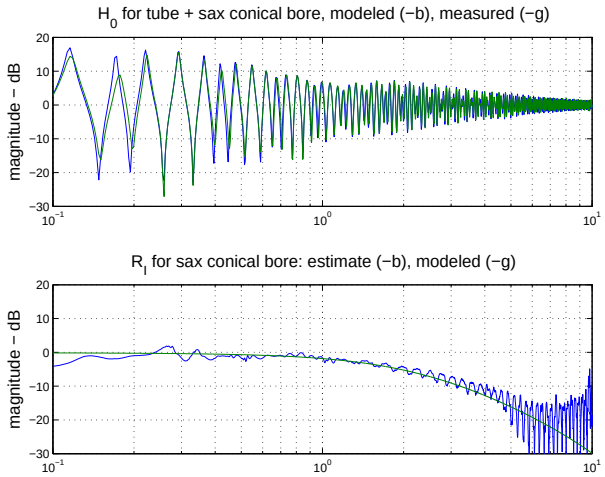


**Figure 6**. A measurement taken of the 2-meter tube with a sax conical bore appended (green), is plotted along with a theoretically constructed model (blue), with the two showing good agreement (top). A good match is also observed for the theoretically constructed round-trip reflection of a cone (green) and that estimated from measurement using (16) (bottom).


### Acknowledgments

We would like to thank the Natural Sciences and Engineering Research Council or Canada (NSERC) and the Canada Council for the Arts (CCA) for their immense support through the joint New Media Initiative program.


## A. CALCULATING TRANSFER FUNCTION OF MEASUREMENT SETUP

The pressure $Y_0(z)$ in Figure 4 corresponding to the measured impulse response (i.e. the actual physical pressure at the microphone) is the sum of the right and left travelling pressure components at the tube's end, that is,

$$Y_0(z) = Y_0^+(z) + Y_0^-(z). \tag{19}$$

The upper (right) travelling component $Y_0^+(z)$ is given by

$$\begin{aligned} Y_0^+(z) &= X(z) + Y_0^+(z)\rho(z)\left(a + c(1 + b + b^2 + ...)\right) \\ &= X(z) + Y_0^+(z)\rho(z)\left(a + \frac{c}{1-b}\right) \\ &= \frac{X(z)}{1 - \rho(z)\left(a + \frac{c}{1-b}\right)}, \end{aligned} \tag{20}$$

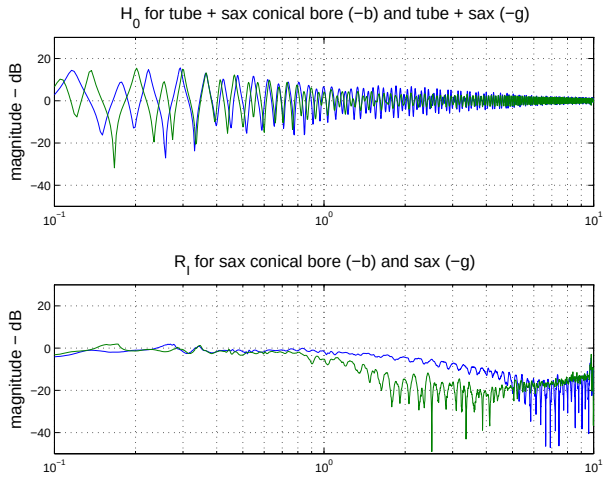


**Figure 7**. The measurement system with the complete sax (green) is shown along with that only having the sax conical bore (blue), with the difference illustrating how the bell shifts the resonant peaks in the spectrum (top). The difference in the round-trip reflection $R_I(\omega)$ of the sax (green) and the conical bore without bell (blue) shows the bell also contributes a low-pass characteristic (bottom).

where $X(z) = \sigma(z)$ is the input speaker transfer function, $a$ is the pressure circulating in the first section,

$$a = R_1(z)\lambda_M^2(z)z^{-2M}, \tag{21}$$

and $b$ is the pressure circulating in the second section,

$$b = R_2(z)R_L(z)\lambda_N^2(z)z^{-2N}, \tag{22}$$

and $c$ corresponds to the outer loop of their connection (the round-trip path from the mouthpiece to the opposite end and back again),

$$c = R_L(z)T_1(z)T_2(z)\lambda_M^2(z)\lambda_N^2(z)z^{-2(M+N)}. \tag{23}$$

The lower (left) travelling component $Y_0^-(z)$ is similarly given by

$$\begin{aligned} Y_0^-(z) &= Y_0^+(z)\left(a + \frac{c}{1-b}\right) \\ &= \frac{X(z)}{1-\rho(z)\left(a + \frac{c}{1-b}\right)} \cdot \left(a + \frac{c}{1-b}\right). \end{aligned} \tag{24}$$

Summing (20) and (24) yields

$$\begin{aligned} Y_0(z) &= Y_0^+(z) + Y_0^-(z) \\ &= X(z)\frac{1 + \left(a + \frac{c}{1-b}\right)}{1-\rho(z)\left(a + \frac{c}{1-b}\right)}, \end{aligned} \tag{25}$$

and dividing by the input $X(z)$ yields the instrument's transfer function $H_0(z)$ given by (13), as measured at the position of the microphone.

## B. REFERENCES


[1] J. O. Smith, "Physical audio signal processing for virtual musical instruments and audio effects," http://ccrma.stanford.edu/~jos/pasp/, December 2008, last viewed 8/24/2009.

[2] A.H.Benade and M.I.Ibisi, "Survey of impedance methods and a new piezo-disk-driven impedance head for air columns," *Journal of the Acoustical Society of America*, vol. 81, no. 4, pp. 1152–1167, April 1987.

[3] J.Kergomard and R.Caussé, "Measurement of acoustic impedance using a capillary: An attempt to achieve optimization," *Journal of the Acoustical Society of America*, vol. 79, no. 4, pp. 1129–1140, April 1986.

[4] T. Ossman, H. Pichler, and G. Widholm, "Bias: A computer-aided test system for brass wind instruments," in *Audio Engineering Society Preprint*, no. 2834, October 1989.

[5] J. Epps, J.R.Smith, and J.Wolfe, "A novel instrument to measure acoustic resonances of the vocal tract during phonation," *Measurement Science and Technology*, vol. 8, pp. 1112–1121, July 1997.

[6] M. M. Sondhi and J. Resnick, "The inverse problem for the vocal tract: Numerical methods, acoustical experiments, and speech synthesis," *Journal of the Acoustical Society of America*, vol. 73, no. 3, pp. 985–1002, March 1983.

[7] J. Agulló, S. Cardona, and D. H. Keefe, "Time-domain deconvolution to measure reflection functions for discontinuities in waveguides," *Journal of the Acoustical Society of America*, vol. 97, no. 3, pp. 1950–1957, March 1995.

[8] V. Välimäki, B. Hernoux, J. Huopaniemi, and M. Karjalainen, "Measurement and analysis of acoustic tubes using signal processing techniques," in *Finnish Signal Processing Symposium (FINSIG'95)*, Espoo, Finland, June 1995.

[9] X. Rodet and C. Vergez, "Physical models of trumpet-like instruments: Detailed behavior and model improvements," in *Proceedings of ICMC 1996*. Clear Water Bay, Hong-Kong: International Computer Music Conference, August 1996.

[10] T. Smyth and J. Abel, "Estimating waveguide model elements from acoustic tube measurements," *Acta Acustica united with Acustica*, vol. 95, no. 6, pp. 1093–1103, 2009.

[11] ——, "Extending the generalized reed model with measured reflection functions," in *Proceedings of ICMC 2007*. Copenhagen, Denmark: International Computer Music Conference, August 2007, pp. 252–255.

[12] T. Smyth and F. S. Scott, "Trombone synthesis by model and measurement," *EURASIP Journal on Advances in Signal Processing*, vol. 2011, no. Article ID 151436, p. 13 pages, 2011, doi:10.1155/2011/151436.